Bright Ideas in Fiber Optics

Incom

LAPPD #31

Measurement & Test Report

August 29, 2018

INCOM, INC.
294 Southbridge Road
Charlton, MA 01507-5238

Tel: (508) 909-2200
Fax: (508) 909-2323

LAPPD #31 Features, Ratings & Performance

LAPPD #31 General Features and Parameters:

Feature	Parameter
Photodetector Material	Borosilicate Glass
Window Material	Fused Silica Glass
Photocathode Material	Multi-Alkali (K_2NaSb)
Spectral Response (nm)	160-650
Wavelength – Maximum Sensitivity (nm)	≤ 365 nm
Photodetector Active Area Dimensions	195mm X 195mm
• Minimum Effective Area	34,989 mm^2 **[(195*195)- {(2*265*6) – (6x6)}]**
• Active fraction with Edge Frame X-Spacers	92% **[(195*195)- {(2*265*6) – (6x6)}] / (195 * 195)**
Anode Data Strip Configuration	28 silver strips, Width = 5.2 mm, gap 1.7 mm, nominal 50 Ω Impedance
Voltage Distribution	5 taps for independent control of voltage to the photocathode and entry and exit of MCP

LAPPD # 31 Operational Ratings

Parameter	Rating
Supply voltage Photocathode — Anode (Volts)	Typical: • 30V between MCP and photocathode • 900-925 V/mcp • 200 V between MCPs • 200 V between MCP and anode • Photocathode voltage is -2230 to -2255 V Maximum: Photocathode voltage at -2900 V
Operating ambient temperature °C	TBD (nominal room temperature)
Storage temperature °C	-12 to 50 (Avoid indium seal melt)

LAPPD Package / Housing Characteristics

Parameter	Rating
Photodetector Physical Dimensions (L X W X Thickness, mm)	230 x 220 x 22
Photodetector Mounting Case	ULTEM or equivalent dielectric polymer
Photodetector Mounting Case Dimensions	243 mm X 274 mm X 25.2 mm
Connectivity	Passive PC Interface Board , (300 mm X 264 mm X 1.6mm)
Overall Footprint, with Mounting Case & PC Interface Board	300 mm X 274 mm X 26.8 mm
Shipping Container	Pelican Case + Cardboard Box + G-force indicators

LAPPD #31 Microchannel Plate (MCP) Features & Performance

MCPs	Two Arranged in a Chevron Pair
Dimensions	203 mm x 203 mm X 1.2 mm
MCP Substrate	Incom C14 Glass
Capillary Pore Diameter (µm) Center to Center Pitch (µm)	20 25
Channel Length / diameter aspect ratio Substrate Thickness (mm)	60:1 1.2
Bias Angle, degrees	13
Capillary Open Area Ratio Percent	68.4
Resistive and Emissive Coatings	Chem 1, Applied via Atomic Layer Deposition (ALD)
Secondary Emission (SEE) Layer Material	MgO
Electrode Penetration – Input & Output (Pore Diameter)	1
MCP ID (Entry / Exit)	C00113-052 / C00113-041
MCP Chevron Pair Gain (@ Measurement & Test)	6.6E6 at 950 V/MCP

LAPPD #31 Operating Performance

Parameter	Performance
MCP resistance in the LAPPD (Entry/Exit)	9.7 / 10.5 Mohms at 900 V E
MCP Dark Rate in the LAPPD (Obtained by setting the photocathode more positive than the entry MCP)	• 0.037 kHz/cm^2 at a threshold of 8E5 gain (134 fC), 925 V/MCP, 30 V positive on photocathode • 0.00015 kHz/cm^2 at a threshold of 8E5 gain (134 fC), 900 V/MCP, 30 V on photocathode [D]
Max Voltage	• 950/950 V/MCP (entry/exit), -2330 volts at the photocathode, or • 900/900 V/MCP (entry/exit), -2400 volts at the photocathode.
Photocathode QE @ 365 nm, max / mean %	14 / 9.8
Photocathode QE Spatial Variability (σ)	1.1%
LAPPD Dark Count rate	• 0.44 kHz/cm^2 at a threshold of 8E5 gain (134 fC), 925 V/MCP, 30 V on photocathode • 0.014 kHz/cm^2 at a threshold of 8E5 gain (134 fC), 900 V/MCP, 30 V on photocathode[D]

LAPPD Gain	8.0 X10^6 @ 925/925 V (entry/exit), 30 V on the photocathode, with variation = σ ≤ 50% mean
Transit Time Variation	99 pS (Provisional: limited by current instrumentation)

Introduction

Functional tests were performed on LAPPD 31 in a dark box that was fitted with a UV light source and signal acquisition hardware. A summary of the results is shown below. The measurements include:

1. **Gain**
   - Gain vs. MCP voltage
   - Gain vs. photocathode voltage
   - Gain vs. repetition rate
2. **Dark rates** vs. MCP and photocathode voltage
3. **Transit Time Variation**
4. **Timing and Position**
   - Position along a strip, inferred from relative pulse arrival times at each end
   - Position across strips from centroiding
5. **Photocathode QE spectrum and map**
6. **MCP resistance vs. voltage**
7. **High voltage connection diagram**

Gain

Gain vs. MCP voltage

Gain was measured as a function of MCP voltage, using PSI DRS4 waveform samplers. MCP pulses were produced by directing a 405 nm Edinburgh Instruments 60 pS UV pulsed laser to a selected point on the LAPPD window. The laser was triggered externally at 13.06 kHz.

A neutral density filter (NE530B from Thorlabs) and a polarization filter were used on the laser to reduce the intensity to the single photon level. At this level, the LAPPD responded to 2 out of every 20 laser pulses.

The gain results are shown in Figure 1 as a function of both MCP and photocathode voltage. The LAPPD gain for single photoelectrons is as high at 9.0E6 at 950 volts/MCP. At MCP voltages of 900 V/MCP or less, the gain tends to increase with increasing photocathode voltages. This is consistent with the expected increase in the number of secondary electrons from the MgO film as incident electron energy rises (Jokela et al., 2012).

At the highest MCP voltages, 950 and 925 V/MCP, the relation of gain to photocathode voltage is the opposite of the other MCP voltages. The average gain decreases with increasing photocathode voltage. This may be a consequence of the increasing dark rates, which increase substantially with photocathode voltage at high MCP voltages (see Figure 6). The increasing dark rates may be in the form of small pulses.

The pulse height distributions are shown in Figure 2, for 30 V on the photocathode and 200 volts on the photocathode. The distributions are well-separated from threshold at 875 V/MCP or more. The gain is as high as 1E7 at 950 V/MCP.

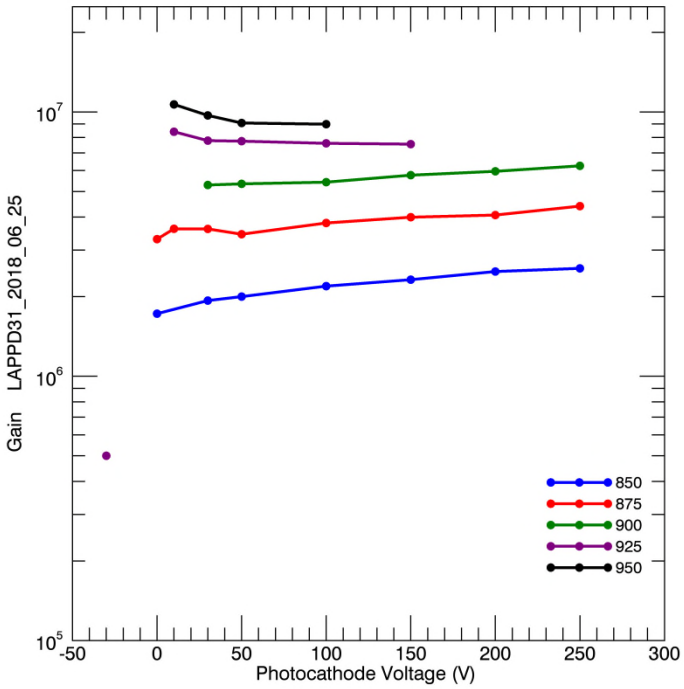

Figure 1: Gain is shown vs. MCP and photocathode voltage, as measured with PSI DRS4 waveform samplers.[A]

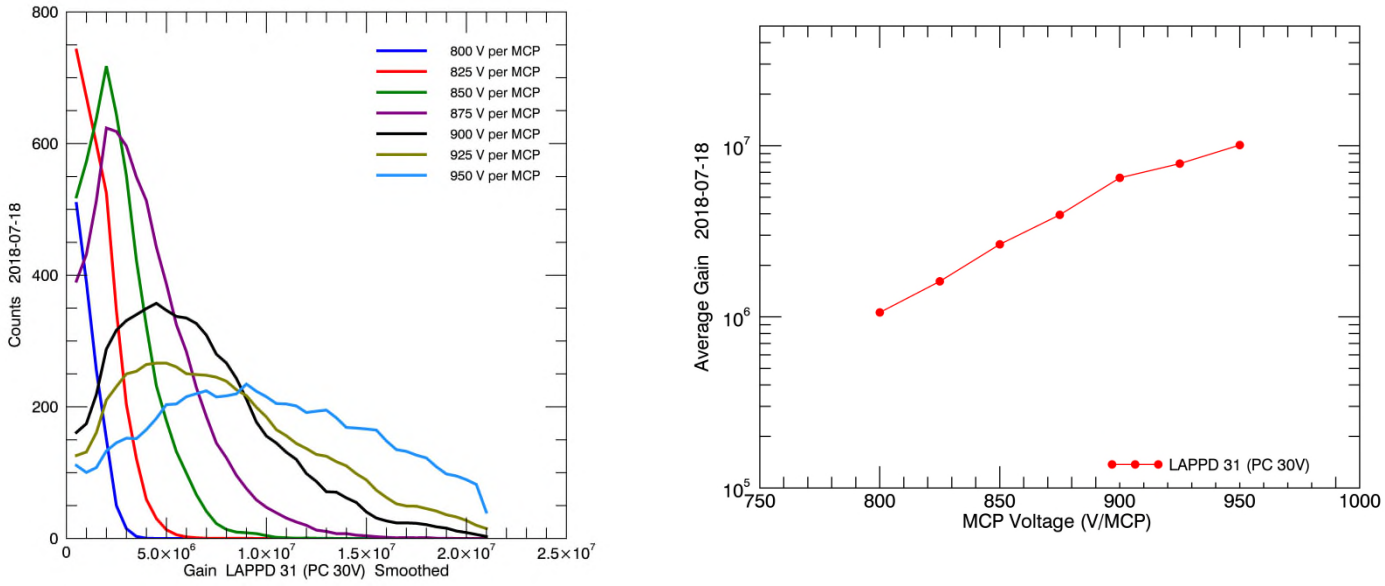

Figure 2: Gain is shown as a function of MCP voltage, with 30 V on the photocathode.[B]

Gain vs. repetition rate

When a microchannel produces a charge pulse, it needs time to recharge. Otherwise, subsequent pulses will be smaller than the first. The microchannel plates are suitable for high rate conditions because the channels are nearly independent of each other, and unless the same one is struck twice, they will have time to recover.

The reduction of gain as a function of rate was tested by applying the 405 nm laser to a spot on the LAPPD window, of about 1 mm in diameter. The repetition rate was changed, and the corresponding gain was measured. The gain in Figure 3 is shown as a function of laser repetition rate. LAPPD 31 responded with 5 out of 20 laser pulses. Figure 4 shows the gain as a function of observed pulse rate, rather than the laser trigger rate. The gain declines by a factor of approximately two as the observed rate is increased from 0.28 kHz to ~17 kHz, or 0.35kHz/mm^2 to ~21 kHz/mm^2: a gain decrease of 10.5E6 to 4.3E6.

This rate is somewhat threshold-dependent, so at higher rates, some pulses fall below threshold. The pulse distributions as a function of laser trigger rate are shown in Figure 5. At higher rates, the pulse height distributions shift to the left, corresponding to reduced gain.

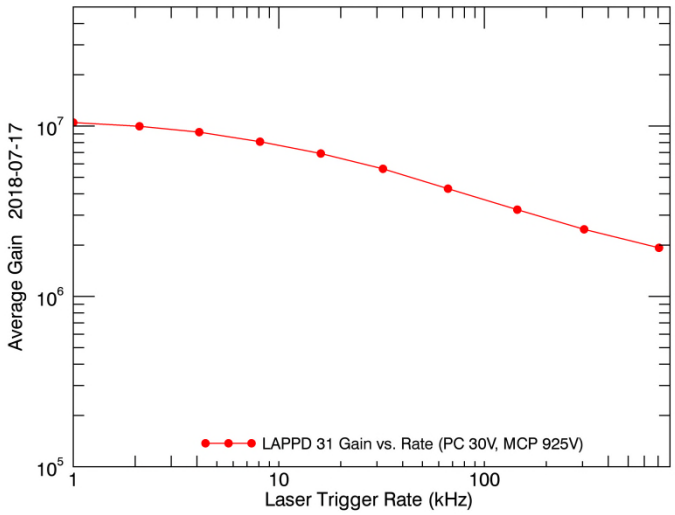

Figure 3: Gain is shown vs. laser repetition rate for single photoelectrons. [C]

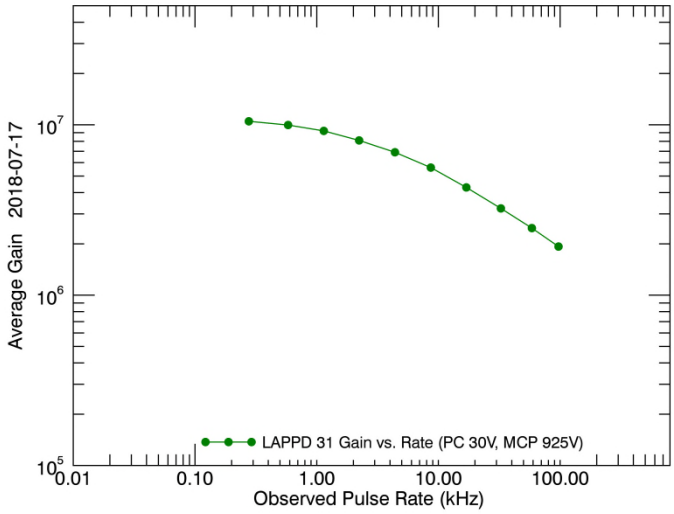

Figure 4: Gain is shown vs. observed pulse rate for single photoelectrons.

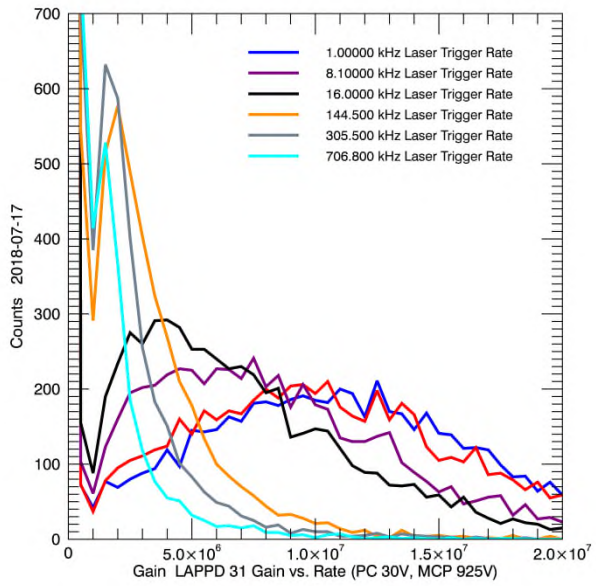

Figure 5: The pulse distributions are shown as a function of laser trigger rate.

Dark rates vs. MCP and photocathode voltage

Dark rates are shown in Figure 6 as a function of MCP voltage and photocathode voltage. The higher photocathode voltages tend to increase the gain, but they also increase the dark rates. These rates were acquired from a single 13.5 cm^2 strip.

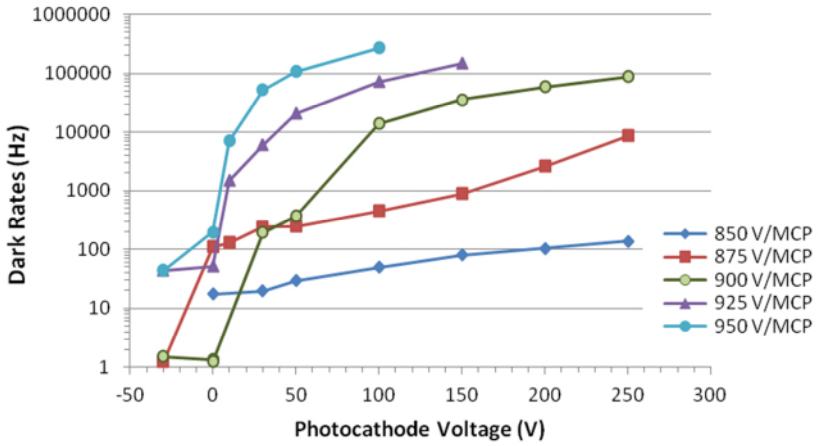

Figure 6: Left - Dark rates are shown as a function of MCP and photocathode voltage. [D]

Transit Time Variation

The time variation between the initiation of a photoelectron and the arrival of the MCP pulse at the end of a strip is of interest for timing applications. This variation represents the timing uncertainty of the LAPPD. The time variation was measured by using a fast photodiode to directly monitor the 405 nm laser pulse. The time difference between the monitor pulse and the corresponding pulse from a single strip was measured using the DRS4 waveform samplers. The variation in this time is the transit time variation of the LAPPD (see Figure 7). Variations may come from phenomena such as the depth to which the photoelectron advances into the microchannel before striking the walls of the channel. Additional variations arise from electronic noise superimposed on the strip measurement, and on the photodiode waveform. There is also a ~±25 pS jitter in the width of the DRS4 timesteps, which is not corrected here. Hence, the quality of the measurement is somewhat environment-dependent, and the result here may not be the best achievable with the LAPPD. These measurements were made with an MCP voltage of 925 V/mcp, and 100 V on the photocathode.

The 405 nm laser that is used for the LAPPD tests has a 60 pS firing window. The intensity is reduced by neutral density filters to produce single photoelectrons. Therefore, the laser photon that produces the single electron may arrive at any time within the 60 pS window. The transit time distribution is shown in Figure 8, left. The standard deviation of the distribution is 116 pS. If the variation of the laser photon has a standard deviation of 60 pS, then the LAPPD transit time variation may be extracted as a sum of squared variations as 99 pS: $\sigma_{Meas}^2 = \sigma_{LAPPD}^2 + \sigma_{LaserWidth}^2$. This is a provisional, likely limited by current instrumentation.

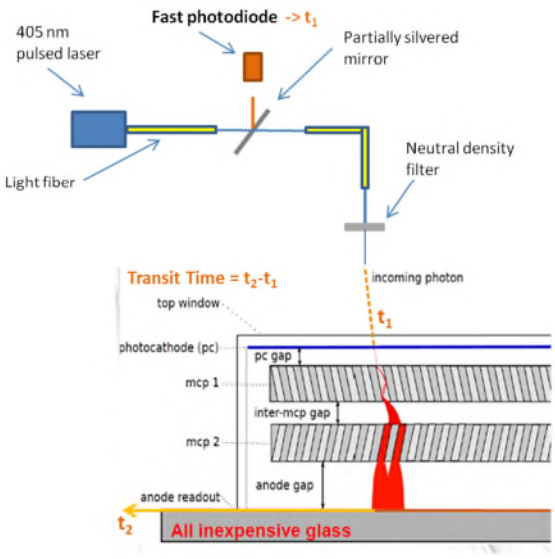

Figure 7: The measurement of the Transit Time Variation is shown.

The Transit Time Variation (TTV) was measured as a function of both MCP and photocathode voltages. The result is shown in Figure 8, right. The TTV decreases at all MCP voltages as the photocathode voltage is increased, up to 100 volts. At higher photocathode voltages, there appears to be no further improvement in time resolution.

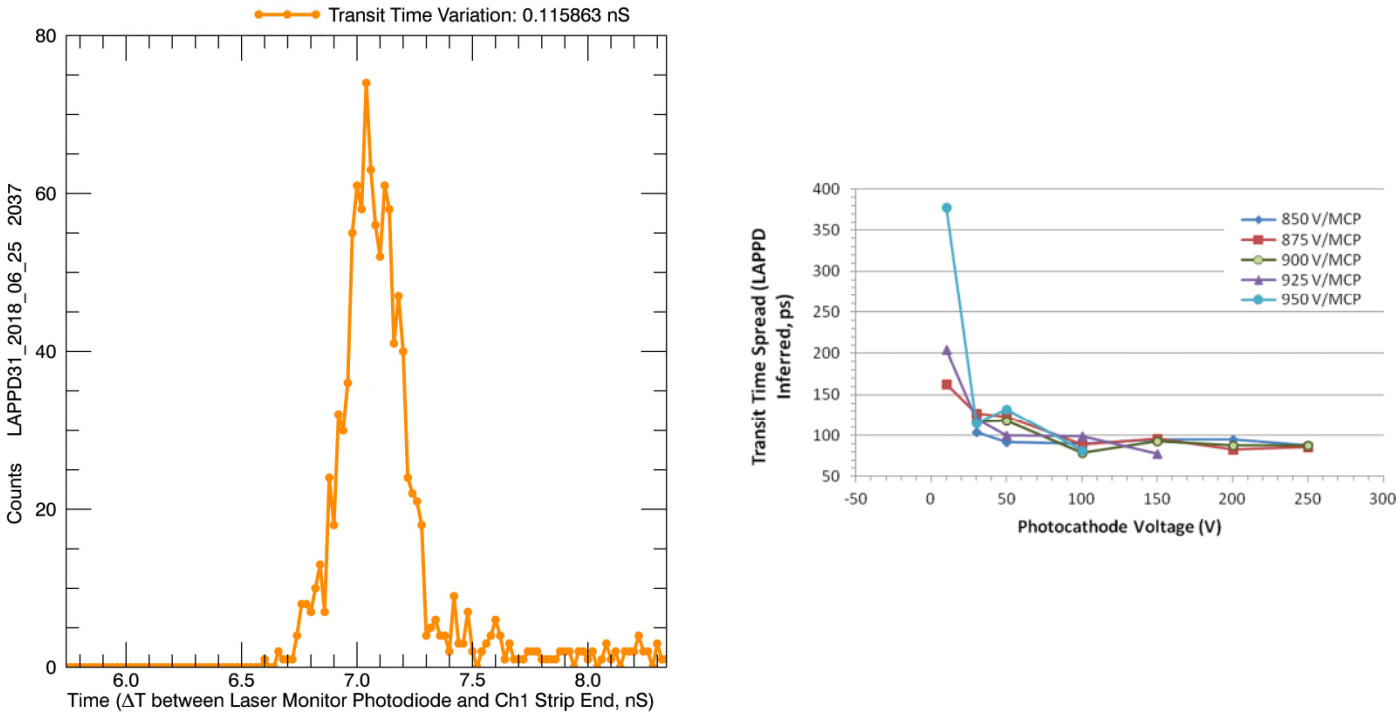

Figure 8: Left - The transit time variation is shown. This is the time difference between the observed laser firing and the arrival of the MCP pulse at the end of an anode strip. Right – the Transit Time Variation is shown vs. MCP and Photocathode voltages.[E]

Position along a Strip

Position may be measured with the LAPPD stripline anode in two ways. Along a strip, the position of the charge pulse may be inferred by measuring the relative time of arrival of pulses at each end of the strip, as the charge deposited by the MCP makes its way to ground at both ends. The time needed for a pulse to travel the entire strip is combined with the difference in arrival time at both ends, and cable offsets are subtracted to calculate the position of charge deposition. This process is shown schematically in Figure 9, right. These measurements were made with MCP voltages of 925 V/mcp, and 30 V on the photocathode. A scan of the 405 nm laser along a strip was observed using a DRS4 waveform sampler at each end of a strip, and the variation in relative timing was measured.

The results of the position scan are shown on the left side of Figure 9. Discontinuities can occur where the laser hits an area of the photocathode with an X-spacer underneath (see Figure 10 right, at the ±10 mm positions). When the laser light is completely obscured this way, the observed position is the average of dark pulses, which tends to be near the center.

.

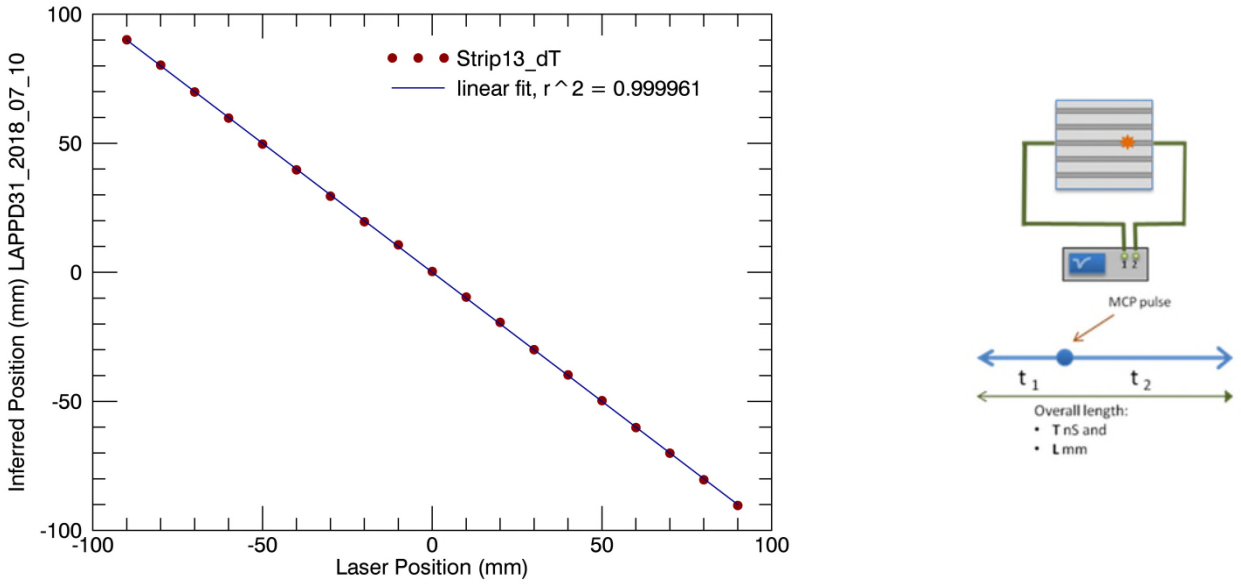

Figure 9: Right - pulses are observed at the left and right ends of a strip, for single photoelectrons. Their relative arrival time leads to position of the charge deposition along the strip.
Left - Position is inferred from average pulse arrival times at each end of a strip, and plotted against the known laser position. [F]

The position resolution along a strip is determined by the arrival time measurement of the pulses at the ends. The inferred position is plotted against the known laser position in Figure 9 (left). The distribution in time differences observed at the ends of one strip, at one position, is shown in Figure 10 (left). The position resolution is inferred from the width of this distribution and is 2.4 mm, at the laser position of 50 mm.

The time variation of this distribution can be calculated for all other positions along the strip. It is shown as a function of position in Figure 10 (right). The large variations at the position ±10 mm is the result of a laser spot landing on an X-spacer, so that only dark pulses contribute to the position measurement.

Another transit was performed with a brighter laser illumination, so the laser pulses produced multiple photons from the photocathode. In this case, every laser firing produced a response from the LAPPD. The position results are shown in Figure 11. The position resolution is somewhat better, at 2.1 mm. An anomalous result is observed at ±10 mm as before, but the time variation at the 0 mm laser position is relatively high.

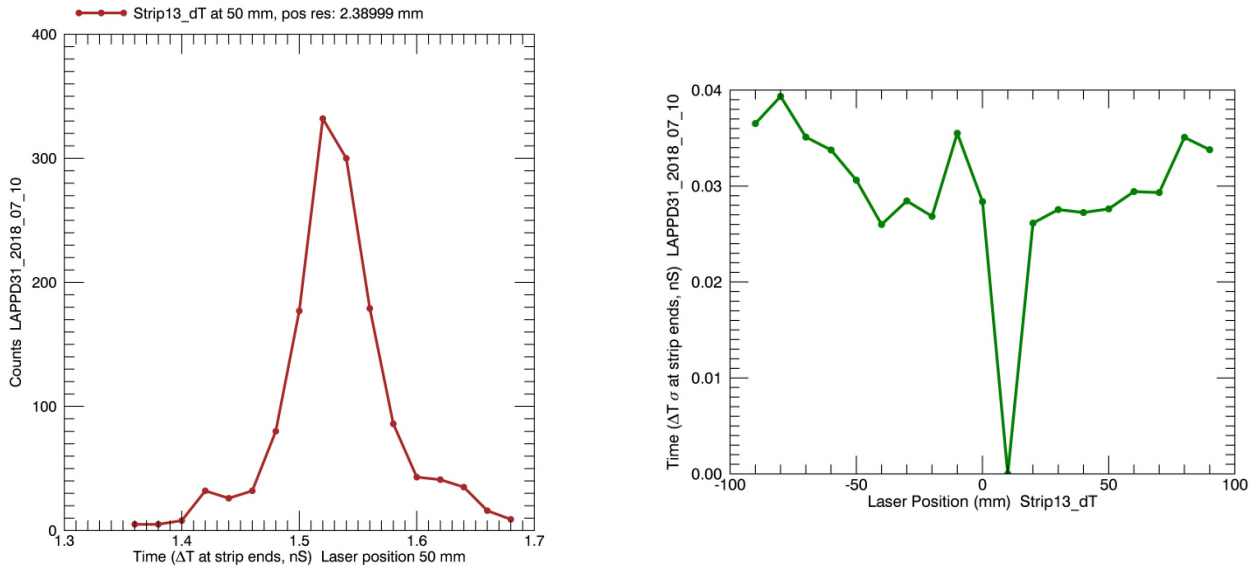

Figure 10: Left - The time distribution is shown for pulses arriving at the ends of a strip, from a laser pulse at the position 50 mm. Right – the width of the time distribution is shown as a function of position along the strip. Note the discontinuity at ±10 mm, where the laser hit an X-spacer.

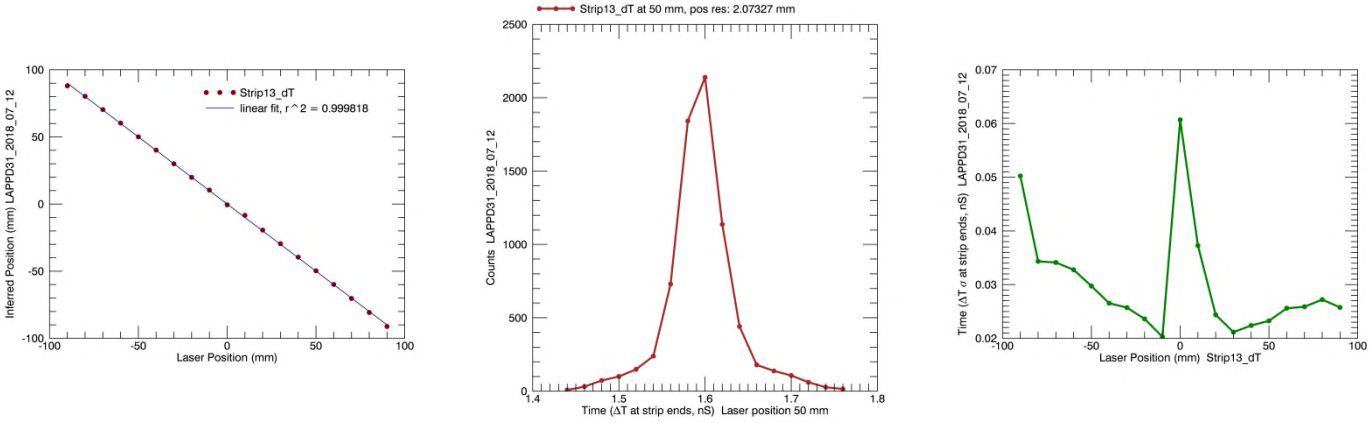

Figure 11: the position is inferred from a multi-photoelectron transit along a strip. Middle: the time differences for pulses observed at the ends of a strip. Right: The time differences as a function of laser position along the strip. The middle panel is drawn from the 50 mm position.[G]

Position Across Strips

Position may be measured across strips as well. In this case, the centroid of five adjacent strip signals may be calculated, resulting in the position to a better resolution than the strip pitch itself. Timing is not used for this position measurement. The relative charge deposition on 5 adjacent strips is shown in Figure 12, as the laser was moved across strips in 1 mm steps. A potential difference of 200 volts was applied between the exit MCP and the anode. The inferred laser position is shown in Figure 13 (left), as inferred from the centroiding. The position resolution is expressed as the deviation from linearity, and is 0.76 mm. A linear fit is superimposed.

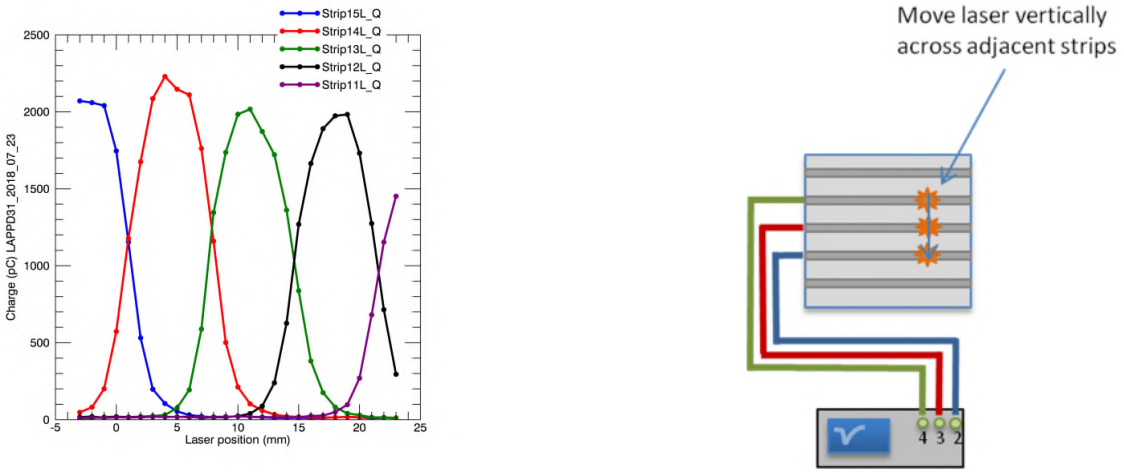

Figure 12: Left - The relative charge distribution among 5 adjacent strips is shown as a function of laser position, with 200 V between the MCP and anode. Right – a sketch of the laser movement is shown. [H]

A transit time measurement was made at the middle strip, 13 (figure 13, right) for reference. Removing the laser pulse width of 60 pS from the sum of the squared uncertainties, the transit time spread was 175 pS. The MCP voltage for this scan was 900 V/MCP, and the photocathode voltage was 30 V. The transit time spread is not optimized until the photocathode voltage is increased to 100 V (see Figure 8).

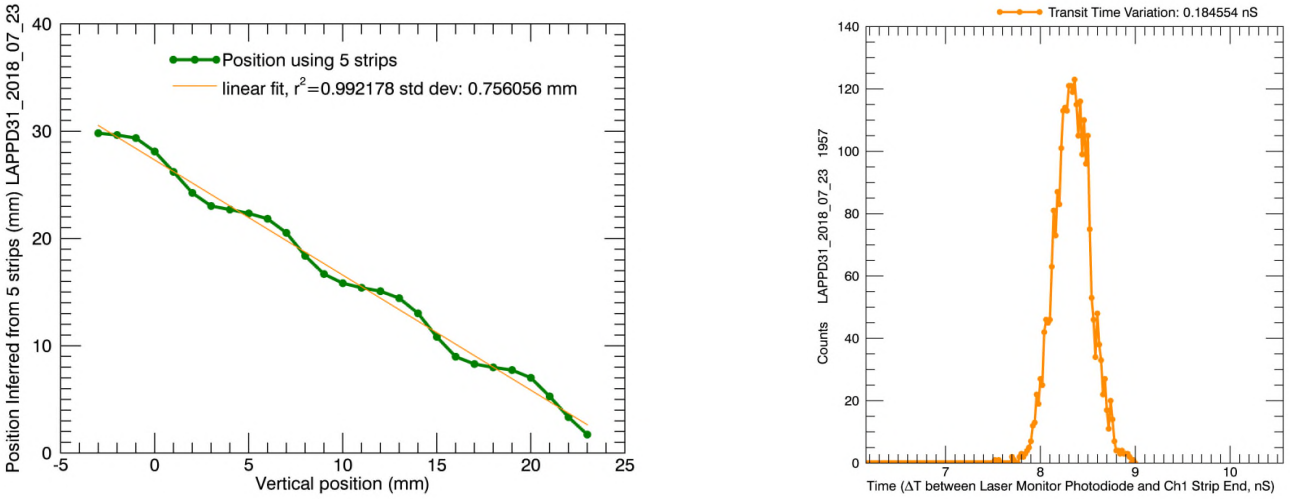

Figure 13: Position as inferred from charge distributions on adjacent strips is shown as a function of laser position.

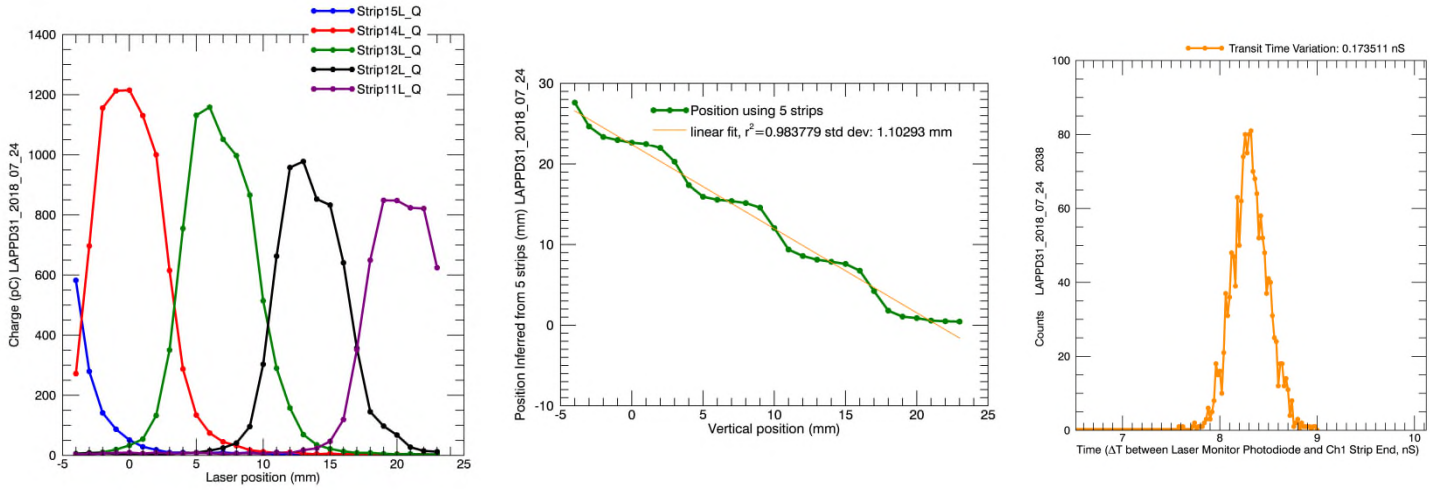

Figure 14: Position and transit time spread are shown for a cross-strip scan with a voltage between the MCP and anode of 50 V. Left: The charge profile on each adjacent strip. Middle: The inferred position at each laser position. Right: The transit time variation at Strip 13. [I]

This position measurement was repeated with only 50 volts between the exit MCP and anode (Figure 14). This weakened the electric field between these two planes. The position resolution became somewhat worse, but the transit time spread became slightly better: 1.1 mm and 163 pS for the 50 volt scan, vs. 0.76 mm and 175 pS from the 200 volt scan.

Photocathode QE spectrum and map

The quantum efficiency of the photocathode was measured across the LAPPD window by scanning a 365 nm UV LED in an XY pattern of 3 mm steps. The illumination on the window had a circular pattern with a ~2.5 mm diameter. The intensity of the input light was measured with a Thorlabs SM1PD2A photodiode, and a Keithley 6485 picoammeter. The photocurrent was collected and measured by connecting both sides of the entry MCP to a Keithley 2400 picoammeter, with a 42 volt bias voltage between the MCP and the photocathode. The quantum efficiency is calculated from the ratio of these two quantities, less the dark current in each.

The UV LED source was stepped across the LAPPD window, and at each step, the input light intensity was measured, as well as the resulting photocurrent. The map is shown in Figure 14. The maximum quantum efficiency is ~14%. The average QE at 365 nm is 9.8%, with a sigma of 1.1% absolute. The X-spacers are visible in the map. The QE is highest in the central region.

The QE spectrum is also shown in Figure 14, from a selected location near the center after the photocathode was manufactured. The highest measured sensitivity is at 365 nm.

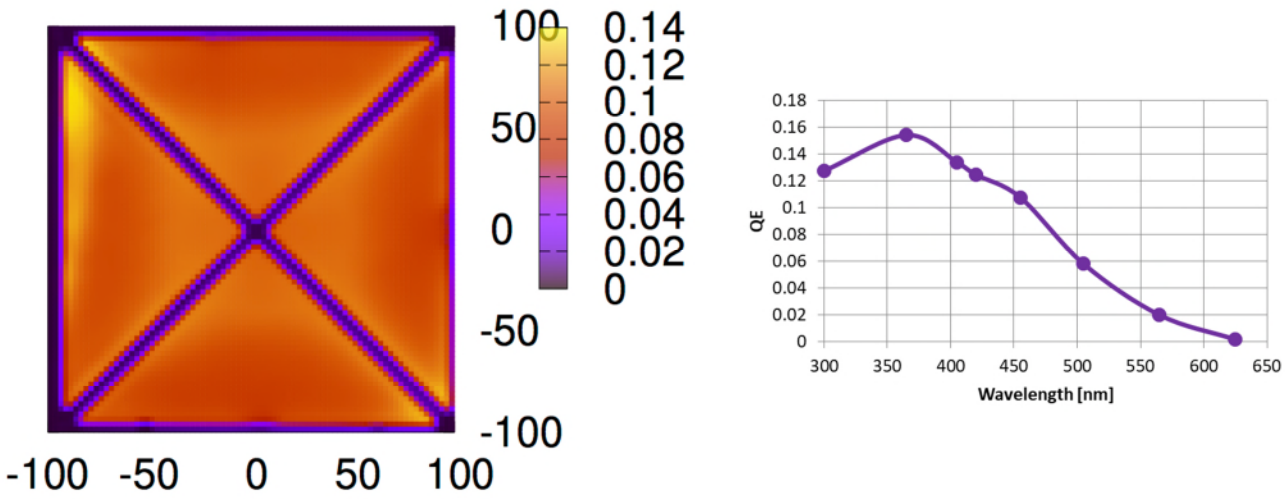

Figure 14: Left: A photocathode Quantum Efficiency map is shown at 365 nm. QE is ~14% at maximum. Right: A QE spectrum is shown at elevated temperature, following fabrication.[J]

MCP resistance vs. voltage

The MCP resistance is shown in Figure 15, as a function of voltage. They are non-ohmic, and their resistance decreases somewhat with increasing voltage. Some of this behavior may be attributed to warming, as the MCP resistance decreases with increasing temperature. The variation of resistance with voltage in Figure 15 must be considered if a resistor divider network will be used to distribute high voltages.

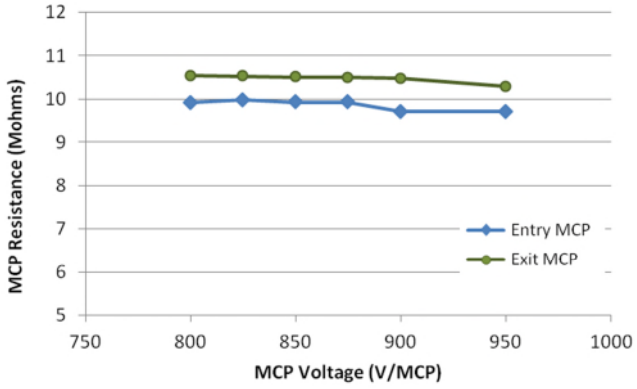

Figure 15: MCP resistances for LAPPD 31.[K]

High voltage connection diagram

The high voltages may be connected as shown in Figure 16 for maximum control of the LAPPD. This approach separates the current paths of the entry and exit MCPs, so anomalies in either may be detected. Additionally, the photocathode voltage may be controlled independently of the MCPs. Without changing the gain, the photocathode voltage may be increased, which will increase the gain somewhat as the photoelectrons acquire more energy before impacting the microchannel. Alternatively, it may be decreased so it is more positive than the entry side of the entry MCP. In this case, the photoelectrons will remain at the photocathode, and the

MCP dark pulses may be observed. This state may also be used if an accidental exposure of the LAPPD to light is anticipated.

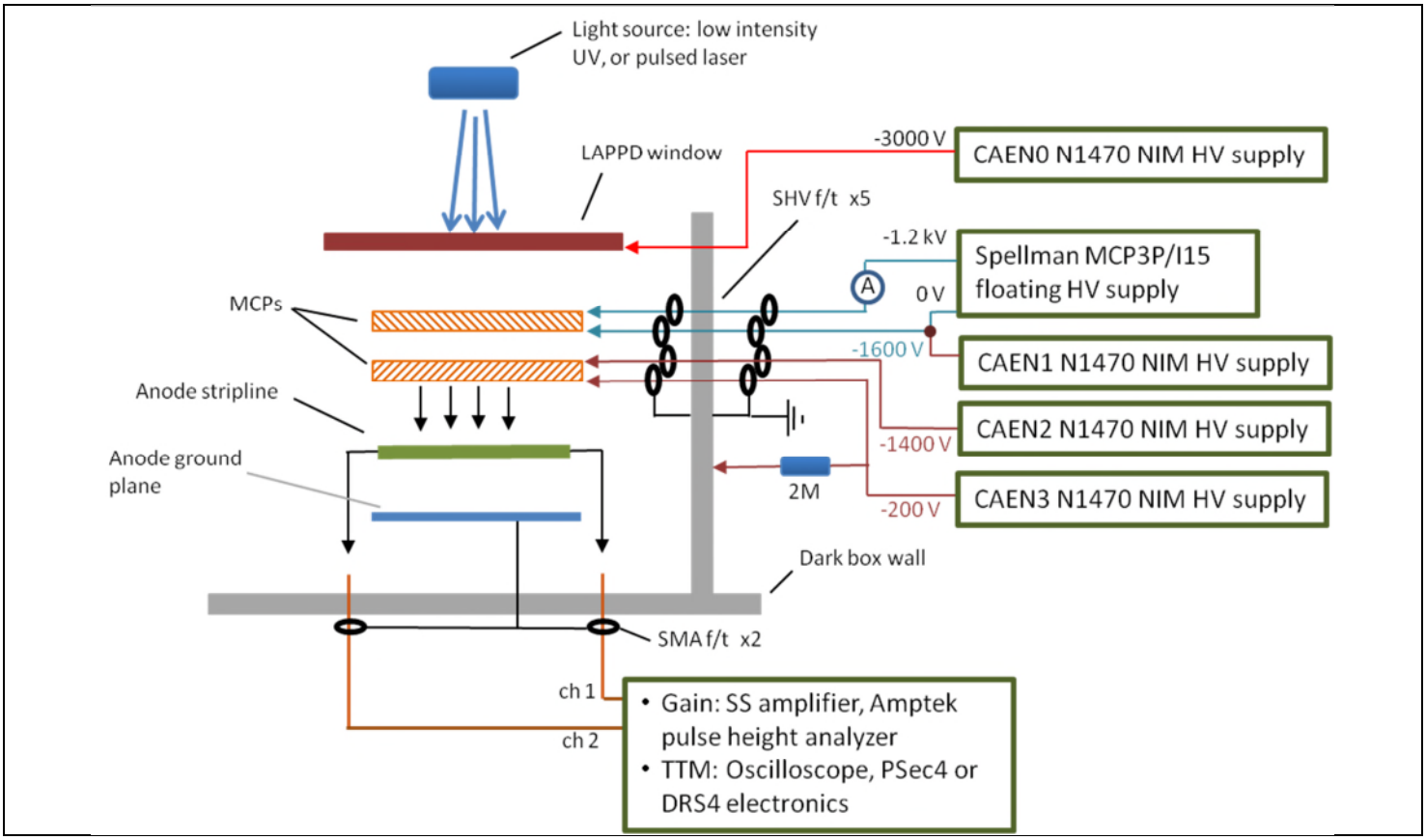

Figure 16: Top - The wiring diagram for high voltage and signals is shown for the LAPPD gain and timing testing at Incom.

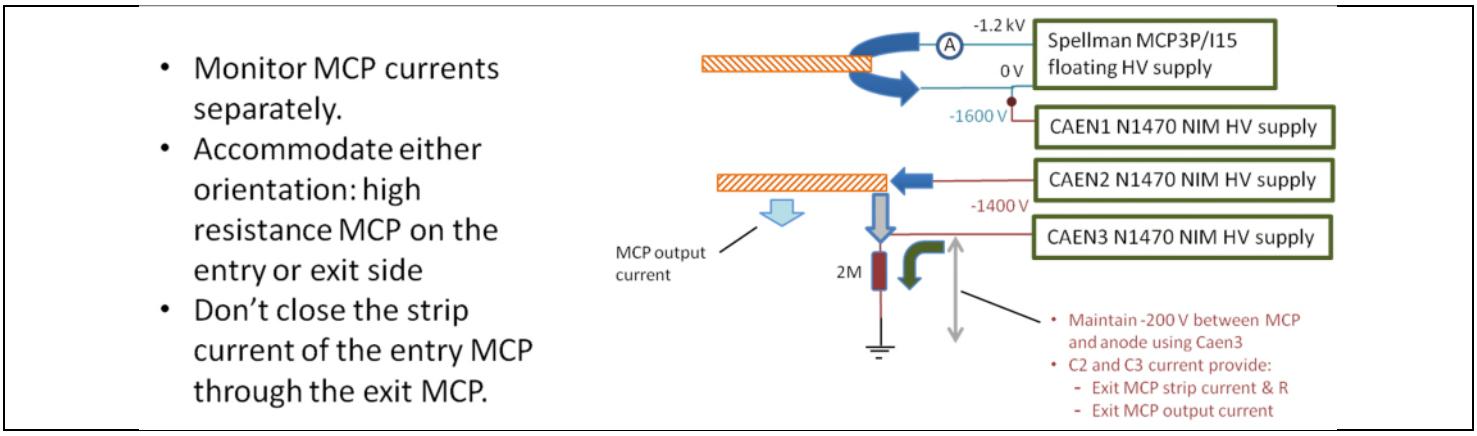

Figure 16: Middle - A schematic shows the separation of the two MCP current paths, and the techniques used to separately measure the output current to the anode and the strip current through the exit MCP.

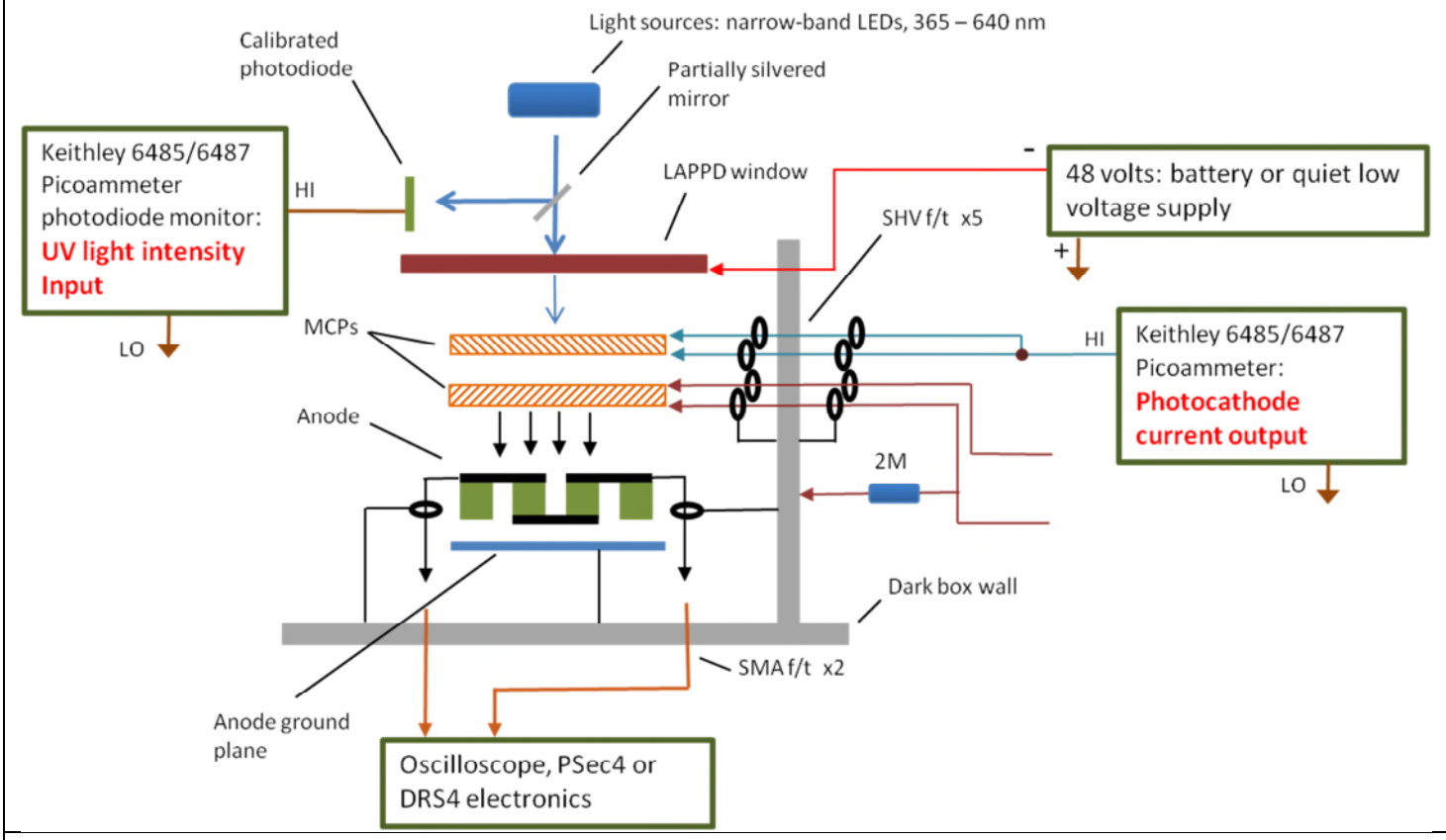

Figure 16: Bottom - The wiring diagram for the QE measurement is shown. The exit MCP and the anode are not involved in this measurement. Instead, the entry MCP serves as the anode for the photocurrent.

Signal and High Voltage Connectivity

An Ultem housing and a backplane are provided with each LAPPD (Figure 17). The backplane connects the strips to SMA connectors with near-50 ohm impedance. The ultem housing provides the high voltage connections. They consist of SHV panel mount connectors on the outside, and Mill-Max spring-loaded ball tip pins on the inside. The pins touch the high voltage pads on the LAPPD envelope. The 5 high voltage connectors are labeled according to their function. The shields on the SHV connectors simply terminate the high voltage cable shield, and minimize unwanted signal pickup in the detector. They do not close any high voltage current paths.

Packing

The LAPPD is wrapped in an antistatic bag and placed in a Pelican case with antistatic foam (Figure 17). The foil helps manage static charging, which could be harmful to charge-sensitive electronics that will be attached to it. It also keeps unnecessary stray light from exciting the photocathode, and charging the entry MCP.

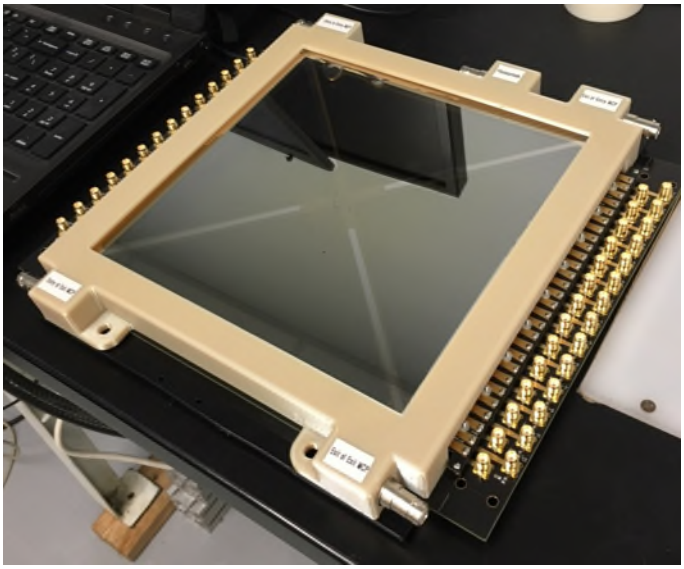

Figure 17: Left - the LAPPD is enclosed in an Ultem housing with high voltage connectors, and mounted on a backplane for signal access. Right - The LAPPD is wrapped in foil to manage static charging, and to keep stray light from the photocathode.

Footnotes

A OnlineMetaData_20180625_Spellman.xlsx
B OnlineMetaData_20180718_Spellman.xlsx
C OnlineMetadata_20180717_Spellman.xlsx
D OnlineMetadata_20180625_Spellman.xlsx
E OnlineMetadata_20180718_Spellman.xlsx
F OnlineMetadata_20180710_Spellman.xlsx
G OnlineMetadata_20180712_Spellman.xlsx
H OnlineMetadata_20180723_Spellman.xlsx
I OnlineMetadata_20180724_Spellman.xlsx
J L:\Engineering\LAPPD-Test-Station\Photocathode scans\LAPPD 31\tile31_QEscan_2018-07-23T7V0_0M.pdf
K OnlineMetadata_20180718_Spellman.xlsx